ELSEVIER

Seminars in
NUCLEAR
MEDICINE

Preclinical Imaging in Targeted Cancer Therapies

Francesca Iommelli, PhD,* Viviana De Rosa, PhD,* Cristina Terlizzi, MS,† Rosa Fonti, MD,* and Silvana Del Vecchio, MD†

Preclinical imaging with radiolabeled probes can provide noninvasive tools to test the efficacy of targeted agents in tumors harboring specific genetic alterations and to identify imaging parameters that can be used as pharmacodynamics markers in cancer patients. The present review will primarily focus on preclinical imaging studies that can accelerate the clinical approval of targeted agents and promote the development of imaging biomarkers for clinical applications. Since only subgroups of patients may benefit from treatment with targeted anticancer agents, the identification of a patient population expressing the target is of primary importance for the success of clinical trials. Preclinical imaging studies tested the ability of new radiolabeled compounds to recognize mutant, amplified, or overexpressed targets and some of these tracers were transferred to the clinical setting. More common tracers such as ^{18}F-Fluorothymidine and ^{18}F-Fluorodeoxyglucose were employed in animal models to test the inhibition of the target and downstream pathways through the evaluation of early changes of proliferation and glucose metabolism allowing the identification of sensitive and resistant tumors. Furthermore, since the majority of patients treated with targeted anticancer agents will invariably develop resistance, preclinical imaging studies were performed to test the efficacy of reversal agents to overcome resistance. These studies provided consistent evidence that imaging with radiolabeled probes can monitor the reversal of drug resistance by newly designed alternative compounds. Finally, despite many difficulties and challenges, preclinical imaging studies targeting the expression of immune checkpoints proved the principle that it is feasible to select patients for immunotherapy based on imaging findings. In conclusion, preclinical imaging can be considered as an integral part of the complex translational process that moves a newly developed targeted agent from laboratory to clinical application intervening in all clinically relevant steps including patient selection, early monitoring of drug effects and reversal of drug resistance.

Semin Nucl Med 49:369-381

Since the approval of imatinib for treatment of chronic myelogenous leukemia, several additional targeted agents were included in the therapeutic armamentarium against cancer. These compounds are monoclonal antibodies or small molecular weight inhibitors that can block the function of critical molecules required for the maintenance of the malignant phenotype. Targeting these molecules with specific inhibitors would cause growth arrest and apoptosis in cancer cells and a benefit for the patient. An example is provided by oncogene drivers, that is, mutant oncogenes that promote malignant transformation in a given organ or tissue. A number of genetic alterations have been identified as triggers of malignant transformation, and the concept of "oncogene addiction" has been introduced to explain the dependence of some cancers from one or few genes for the maintenance of their malignant phenotype.[1,2] Once the oncogene driver of a specific neoplasm has been identified, it becomes an optimal target for therapy since its inhibition causes cell death.

*Institute of Biostructures and Bioimaging, National Research Council, Naples, Italy.
†Department of Advanced Biomedical Sciences, University of Naples "Federico II", Naples, Italy.
Address reprint requests to Silvana Del Vecchio, Department of Advanced Biomedical Sciences, University of Naples "Federico II", Edificio 10, Via S. Pansini, 5, Naples 80131, Italy. E-mail: delvecc@unina.it

https://doi.org/10.1053/j.semnuclmed.2019.06.003
0001-2998/

Despite the success achieved by several compounds, many targeted anticancer drugs failed to get clinical approval because they did not meet endpoints of clinical trials. Critical analysis of such failures lead to the identification of several important issues that need to be addressed in early drug development including target expression, patient selection, pharmacokinetics, pharmacodynamics, and drug resistance.[3,4] Preclinical imaging studies can provide noninvasive tools to evaluate drug target expression, its functional modulation, tumor targeting, pharmacokinetic, and pharmacodynamic aspects thus identifying the compounds that have a high probability of success in the subsequent experimental clinical phases. Furthermore, preclinical imaging studies can identify and validate imaging parameters that can be translated into the clinical context and used as pharmacodynamics markers in patients treated with targeted agents. The present review will primarily focus on preclinical imaging studies that can be helpful to accelerate the clinical approval of targeted agents and to develop imaging biomarkers for clinical applications. Due to space constraints, we cannot provide an overview of all the target/agent systems developed so far but we will provide representative examples of how preclinical imaging studies may help to select patients for targeted therapies, to monitor drug effects during treatment, and to identify and overcome drug resistance.

Target Expression

Targeted agents bind to molecules that are expressed in tumors bearing specific genetic alterations and hence only subgroups of patients may benefit from treatment with these agents. Therefore, the identification of a patient population expressing the target is a critical early step in all clinical trials. Depending on the specific genetic alterations and molecular landscape of a given tumor, several molecular, genetic, and histopathologic tests are currently used to identify subgroups of patients who will likely respond to therapy.[3,5] Preclinical studies were performed to test the ability of new tracers to recognize mutations or aberrant expression of targets in living organisms providing information on their levels within tumors, distribution in the whole body, and eventually highlighting heterogeneity among tumor lesions (Table 1).

An example is provided by EGFR, a well-recognized oncogene driver of non−small cell lung carcinoma (NSCLC). The most common activating mutations in the kinase domain of EGFR are exon 19 deletions and exon 21 missense mutation (L858R). These mutations occur in 10%-15% of Caucasian and 30%-40% of Asian NSCLC patients and are associated with an increased sensitivity to EGFR tyrosine kinase inhibitors (TKIs). These are small molecules that compete for the ATP binding to the catalytic kinase domain of EGFR thus

Table 1 Representative Radiolabeled Probes Recognizing Main Oncogene Drivers in Preclinical Animal Models

Target	Tracers	Scan Time p.i.	Animal Model	Ref
EGFR	**Small molecules**			
	[^{11}C]PD153035	≤60 min	Lung cancer	(6)
	[^{11}C]erlotinib	≥10 min, ≤90 min	Lung, colon, and glioblastoma cancer	(7-9)
	[^{18}F]gefitinib	1 h	glioblastoma and lung cancer	(10)
	[^{18}F]afatinib	≤2 h	NSCLC	(11)
	[^{11}C]osimertinib	≤2 h	Cynomolgus monkeys	(12)
	[^{18}F]F-PEG6-IPQA	≤3 h	NSCLC with wild type and mutant EGFR	(13)
	[^{18}F]IRS	1 h, 2 h	NSCLC	(14)
	[^{18}F]ODS2004436	≤3 h	Lung cancer	(16)
HER2	**Antibody/protein-based**			
	[^{89}Zr]trastuzumab	48 h	Breast and ovarian cancer	(17,18,24,25)
	[^{111}In]-, [^{64}Cu]DOTA-trastuzumab Fab	24 h		
	[^{124}I]C6.5 diabody	≤24 h, 48 h	Breast and ovarian cancer	(22,23)
	[^{68}Ga]NOTA-2Rs15d		Ovarian and breast cancer	(27-29,32)
	[^{18}F]FB-2Rs15d	1 h		
	[^{18}F]RL-I-5F7	≤4 h, 24 h		
	[^{131}I]SGMIB-2Rs15d			
	[^{18}F]$Z_{HER2:342}$	1 h, 4 h	Breast and ovarian cancer	(26,30,31)
	[^{111}In], [^{68}Ga]DOTA- $Z_{HER2:2395}$			
	[^{111}In], [^{68}Ga]NODAGA-$Z_{HER2:2395}$			
	[^{188}Re]$Z_{HER2:V2}$			
c-MET	**Antibody/protein-based**			
	[^{76}Br]onartuzumab	≥24 h, ≤5 days	Gastric and glioblastoma cancer	(36,38)
	[^{89}Zr]onartuzumab			
	[^{89}Zr]DN30			
	[^{89}Zr]minibody	24 h, 44 h	Lung cancer	(37)
	[^{89}Zr]H2 cys-diabody	4 h, 20 h		
	[^{18}F]AH113804	1 h	Breast and gastric cancer	(39,40)
	[^{99m}Tc] AH-113018	60 min, 90 min		
	[^{89}Zr]PRS-110	≥6 h, ≤96 h	Lung, ovarian, and glioblastoma cancer	(41)

inhibiting receptor autophosphorylation and downstream signaling. The presence of activating mutations is currently considered as a prerequisite to candidate patients with advanced NSCLC to first-line therapy with EGFR TKIs. Although first-generation reversible inhibitors such as gefitinib and erlotinib provided significant clinical benefit, the occurrence of drug resistance prompted the development of new irreversible inhibitors. Among these, osimertinib selectively inhibits EGFR with activating mutations even in the presence of the acquired secondary T790M mutation that is the most common cause of resistance in NSCLC patients treated with EGFR TKI.

Several tracers were developed based on the chemical structure of TKIs and were labeled with ^{11}C and ^{18}F (Table 1). The ability of these tracers to recognize mutant EGFR is thought to be determined by their higher affinity for the kinase domain harboring activating mutations as compared to the wild type domain. Among these probes, ^{11}C-PD153035, a quinazoline derivative based on reversible TKI, was tested in nude mice bearing NSCLC.[6] PET-CT imaging studies showed that tracer uptake was higher in sensitive xenografts harboring activating EGFR mutations than in resistant xenografts with wild type or double mutant (L858R/T790M) EGFR. Furthermore, tumor-to-nontumor ratios were positively correlated with phospho-EGFR levels in sensitive xenografts but not in resistant xenografts.

Other imaging probes including ^{11}C-erlotinib,[7–9] ^{18}F-gefitinib,[10] and ^{18}F-afatinib[11] were obtained by labeling the drug itself and when tested in animal tumor models, ^{11}C-erlotinib and ^{18}F-afatinib showed a higher uptake in tumors with mutant EGFR than in those with wild-type receptor. The advantage to use these tracers in patients is that they can provide additional information on drug pharmacokinetics. For instance, osimertinib was labeled with ^{11}C and used in a nonhuman primate model to evaluate pharmacokinetics and brain penetration.[12] PET imaging studies showed a greater accumulation of ^{11}C-osimertinib in the brain as compared to ^{11}C-gefitinib and ^{11}C-rociletinib indicating its potential clinical efficacy in the treatment of brain metastases of NSCLC.

Among the tracers specifically designed to recognize mutant EGFR, ^{18}F-PEG6-IPQA had an increased selectivity and irreversible binding to active mutant L858R EGFR.[13] PET studies in animal models showed that ^{18}F-PEG6-IPQA was able to discriminate NSCLC xenografts bearing L858R mutant EGFR from those expressing wild-type EGFR. Similar results were obtained with another PET tracer, ^{18}F-IRS, which was able to selectively bind to mutant EGFR bearing exon 19 deletion.[14] Imaging studies showed a high uptake of ^{18}F-IRS in xenografts with mutant EGFR at 120 minutes post injection and the administration of gefitinib significantly reduced tracer accumulation. The same group employed an analogous radiolabeled probe in a first-in-human PET-CT imaging of NSCLC patients and a high tracer uptake was found in tumors harboring EGFR-activating mutations as compared to tumors with wild-type EGFR.[15] Recently, a new compound, ODS2004436, was labeled with ^{18}F and tested for its ability to bind activated EGFR both in vitro and in animal tumor models.[16] In addition to a high affinity for the mutant EGFR in vitro, this new radiolabeled compound showed a high tumor uptake in lung cancer xenografts bearing mutant L858R EGFR, whereas tumor uptake was low in the absence of activating mutations. Furthermore, a good correlation was found between radiotracer uptake in tumors and phospho-EGFR immunostaining, suggesting that ^{18}F-ODS2004436 is a good biomarker of activated EGFR, regardless of the mutation.

Oncogene drivers may also be the results of overexpression or amplification of certain genes. High levels of HER2 occur in approximately 20% of breast and esophagogastric cancers mainly due to gene amplification and are able to drive tumor growth and proliferation. The expression and amplification of this gene usually is assessed by immunohistochemistry and fluorescence in situ hybridization of the surgically excised tumor and the results of such assays will candidate the patient to treatment with HER2 targeted agents. However, in the metastatic setting, it is not possible to perform biopsy on each lesion especially when they are not easily accessible. Therefore, several imaging agents were developed based on the molecular structure of trastuzumab, a humanized monoclonal antibody recognizing the extracellular domain of the transmembrane receptor HER2. The whole monoclonal antibody was labeled with ^{89}Zr and used in animal models and in patients with metastatic breast cancer or esophagogastric cancer.[17–21] To improve pharmacokinetics, engineered antibody fragments such as antigen-binding, single chain variable fragments, diabodies, and minibodies recognizing HER2 were labeled with ^{124}I[22,23] or ^{64}Cu[24,25] and used to perform PET studies in animal models of several tumors including breast and ovarian cancer. Promising imaging agents are camelid single-domain antibody fragments and several nonimmunoglobulin protein scaffolds such as affibodies that are reported to have a more advantageous pharmacokinetics, biodistribution, and tumor homing properties as compared to intact monoclonal antibodies. Single-domain antibody fragments (nanobodies) and affibodies recognizing HER2 were labeled with a variety of radionuclides including ^{18}F,[26–28] ^{68}Ga,[29,30] ^{111}In,[30] ^{188}Re,[31] and ^{131}I[32] for PET and SPECT studies. Imaging with these tracers was reported to successfully detect different HER2 levels in breast and ovarian cancers showing a high tumor-to-background ratios and a good correlation of imaging findings with biodistribution estimates of tumor tracer concentration and receptor expression.

Amplification of MET gene is one of the mechanisms that can cause the constitutive activation of this receptor resulting in oncogene-driven tumorigenesis. MET is a receptor tyrosine kinase that, upon binding to its ligand hepatocyte growth factor (HGF), activates a signaling cascade mainly mediated by the RAS-MAPK, PI3K-AKT, and STAT/JNK pathways responsible for cell-cycle progression, survival, and enhanced cell motility. Aberrant expression or constitutive activation of MET was found in a variety of cancers including NSCLC,[33] renal,[34] and ovarian cancer.[35] MET amplification can be intrinsically present in primary untreated tumors and/

or emerge as a compensatory mechanism in cancers exposed to inhibitors of other oncogene drivers such as EGFR TKIs (see section on "Reversal of drug resistance").

Several imaging agents recognizing MET have been developed and tested in animal models. Monoclonal antibodies and human diabody fragments labeled with ^{89}Zr or ^{76}Br showed a specific enhanced uptake in tumors with high levels of MET as compared with xenografts with low MET expression.[36-38] Furthermore, MET-binding peptides showing a more rapid pharmacokinetic profile as compared to antibody-based compounds were labeled with ^{18}F and ^{99m}Tc for PET and SPECT imaging, respectively.[39,40] Other protein-based small imaging probes such as anticalins with monovalent specificity for MET were generated and labeled with ^{89}Zr.[41] A specific and significant higher tumor uptake was observed in MET-overexpressing xenografts as compared to MET-negative tumors at 48 hours post injection. Despite the development of several promising tracers recognizing MET, the molecular status of MET should be known for the enrollment of patients in clinical trials targeting this receptor. In fact, previous studies showed that only tumors harboring MET genetic lesions, mainly amplification, have a good response to MET inhibition characterized by growth arrest, apoptosis, and tumor regression.[42] Genomic profiling of single tumors can identify these genetic lesions recognizing MET as the oncogene driver in the molecular landscape of that tumor.

Early Monitoring of Tumor Response

Preclinical imaging studies evaluating early tumor response to a new targeted agent can provide evidence that the new compound is able to induce functional changes into the cellular and biological processes modulated by the target. Therefore, by testing the efficacy of several compounds, preclinical imaging may identify those that can move on the following experimental phases. Preclinical imaging studies are designed to allow visualization of drug-modulated processes in basal conditions and early in the course of treatment. The selection of the tracer depends on the target, downstream pathways, and modulated processes. For instance, treatment with EGFR TKIs by inhibiting EGFR signaling induces growth arrest of tumor cells in G1 phase of the cell cycle and a reduction in the rate of proliferation at very early time points. Visualization of proliferation with radiolabeled thymidine analogs such as ^{18}F-fluorothymidine (^{18}F-FLT) before and few days after the beginning of treatment with these agents was employed in previous studies to test drug efficacy in several animal models.[43,44] The common finding of imaging studies performed in sensitive tumors before and after treatment with EGFR TKIs was a marked reduction of ^{18}F-FLT uptake occurring very early in the course of therapy (within 24-48 hours) when tumor size was still unchanged (Fig. 1). Conversely, refractory tumors showed an unchanged or even increased ^{18}F-FLT uptake at the same time points. Similar results were

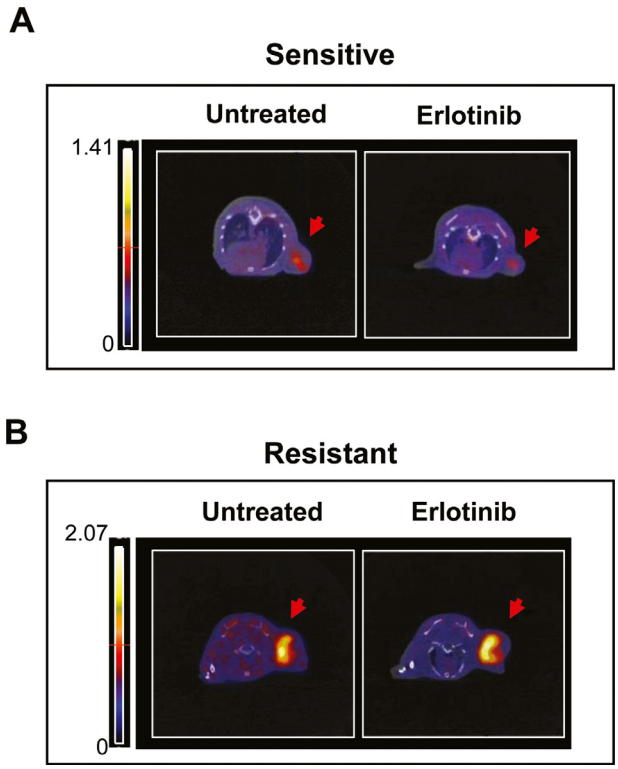

Figure 1 ^{18}F-FLT PET-CT imaging of sensitive and resistant oncogene-driven NSCLCs before and after treatment with erlotinib. (A and B) Representative transaxial fusion PET-CT images obtained from untreated and erlotinib treated HCC827 xenografts bearing activating EGFR mutation and resistant H1975 xenografts harboring T790M mutant EGFR. ^{18}F-FLT PET-CT scan was performed at baseline and after 3 days treatment with 150 mg/kg erlotinib. A decrease of ^{18}F-FLT uptake was observed in sensitive tumor, whereas an increase of tracer uptake was found in resistant tumor.

obtained in preclinical imaging studies with ^{18}F-FLT in animal models treated with a number of targeted agents including PI3K/AKT/mTOR,[45–53] MEK 1/2,[54–57] BRAF,[58–60] MET,[61–63] Aurora kinase,[64–66] and histone deacetylase inhibitors[67–70] (Table 2). In a meta-analysis including 147 studies using ^{18}F-FLT to monitor treatment response in animal models, 83% of the studies reported a decline of ^{18}F-FLT uptake after therapy.[43] An association between ^{18}F-FLT uptake and the rate of proliferation as assessed by Ki67 immunostaining in tumor samples was reported.[71–73] Validation of imaging findings of ^{18}F-FLT PET in animal models was obtained also by analyzing the levels of signaling mediators downstream the target in excised tumors after treatment in comparison to those of untreated animals.[62] Interestingly, in a small percentage of studies (8%), the administration of agents that inhibit thymidylate synthase such as capecitabine was reported to cause an increase of ^{18}F-FLT uptake due to an upregulation of thymidine salvage pathway.[74,75] Therefore, the mechanism of action of the targeted agent should be taken into account when using ^{18}F-FLT since the tracer enter cancer cells through the thymidine salvage pathway that can be modulated by the drug.

Table 2 Selected Preclinical Imaging Studies With ^{18}F-FLT PET in Different Animal Models

Target	Drug	Animal Model	Ref
EGFR			
	Erlotinib	Lung, epidermoid and H&N cancer	(62,99-101,107)
	Cetuximab	Lung and colorectal cancer	(71,101,108)
	CL-387,785	Lung cancer	(100)
	WZ4002	Lung cancer	(100)
PI3K/AKT/mTOR			
	Everolimus	Lymphoma, lung, colorectal, and ovarian cancer	(45-48)
	BEZ235	Glioblastoma and gastric cancer	(49,50)
	AZD8055	Glioblastoma	(52)
	Temsirolimus	Burkitt lymphoma	(53)
MEK1/2			
	PD0325901	Melanoma, breast, and colorectal cancer	(54-56)
	Selumetinib	Colorectal cancer	(57)
BRAF			
	PLX4720	Colorectal and melanoma	(58-60)
	PLX3603		
MET			
	Crizotinib	Lung, glioblastoma, and gastric cancer	(61,62,107)
	BAY 853474	Gastric cancer	(63)
Aurora kinase			
	TAK-901	Colorectal cancer	(64)
	BMS-754807	NSCLC	(65)
	AZD1152	Colorectal cancer	(66)
HDAC			
	Belinostat	Ovarian and colon cancer	(67,68)
	Vorinostat	Hepatoma and colon cancer	(69,70)

The effects of targeted agents were also monitored with ^{18}F-FDG in animal models. The rationale to use ^{18}F-FDG in the early detection of response to targeted agents relies on the fact that oncogene-driven tumorigenesis implies the reprogramming of key regulatory steps of energy metabolism in cancer cells that become highly dependent on aerobic glycolysis rather than on mitochondrial oxidative phosphorylation. The inhibition of the oncogene driver by targeted agents causes an early metabolic switch from aerobic glycolysis to mitochondrial oxidative phosphorylation.[76] This is accomplished by a dramatic reduction of hexokinase II and phospho-pyruvate kinase M2 levels and an upregulation of mitochondrial complex subunits. Cancer cells become less dependent from glucose supply and ^{18}F-FDG uptake is reduced a few hours or days after drug administration when cell viability is still unchanged. Therefore, when detected very early in the course of treatment with targeted agents, reduction of ^{18}F-FDG uptake may reflect inhibition of the target although this does not always predict the final response to treatment with a given targeted agent. In fact, if oncogene-driven tumor cells develop resistance to the targeted agent during treatment, a reduction of glucose metabolism is still possible depending on the new configuration of the signaling network while proliferation remains under the unique control of the oncogene driver. Other confounding situations may occur when the selected target is not the oncogene driver of a given tumor. Depending on the role of the target in the signaling network, its inhibition can reduce glucose metabolism while proliferation continues to be orchestrated by the unaffected oncogene driver. Alternatively, ^{18}F-FDG uptake can be unchanged independently from proliferation and in this case imaging studies at later time points are needed to assess whether cell viability is declined or not in response to the drug. In fact, it is well known that imaging studies with ^{18}F-FDG performed several weeks after the initiation of therapy mainly reflect tumor cell viability and have a high predictive value on the final response to treatment.

Preclinical imaging studies with ^{18}F-FDG were performed in animal models before and early after treatment with a number of targeted agents including EGFR,[76–82] Pan-HER,[83,84] c-kit,[85–87] VEGF A/VEGFR,[88–91] PI3K/AKT/mTOR,[47,48,53,92,93] MEK 1/2,[57,94,95] BRAF,[58,59,96] and histone deacetylase inhibitors[68,97] (Table 3).

The majority of these studies reported the reduction of ^{18}F-FDG at approximately 1-8 days from treatment initiation. When the targeted agent is a monoclonal antibody, its effect on glucose metabolism is expected to occur at later time points as compared to treatment with small inhibitors. This is because large molecules such as monoclonal antibodies are able to reach and bind to their targets several days post injection, whereas small inhibitors have a more rapid pharmacokinetic profile. For instance, mice bearing HER2-overexpressing xenografts showed a reduction of ^{18}F-FDG uptake after 16 days of treatment with trastuzumab, whereas no changes of ^{18}F-FDG uptake were observed in tumors with low levels of HER2 during the entire course of therapy.[98]

Table 3 Selected Preclinical Imaging Studies With ^{18}F-FDG PET in Different Animal Models

Target	Drug	Animal Models	Ref
EGFR			
	Erlotinib	Lung and H&N cancer	(76-79)
	Gefitinib	Lung cancer and epidermoid carcinoma	(80,81)
	WZ4002	Lung cancer	(76)
	Cetuximab	SCCHN PDX models	(82)
Pan-HER			
	Canertinib	Epidermoid carcinoma	(83)
	Antibody mixture	Pancreatic carcinoma	(84)
c-kit			
	Imatinib	GIST	(85-87)
VEGF-A/ VEGFR			
	Axitinib	Breast and glioblastoma	(88)
	Bevacizumab	Rhabdomyosarcoma, breast, and glioblastoma	(89-91)
PI3K/AKT/ mTOR			
	AZD8186	Renal, breast and glioblastoma	(92)
	Temsirolimus	Burkitt lymphoma	(53,93)
	Everolimus	Lung, colorectal cancer, and GIST	(47,48,86)
MEK1/2			
	Selumetinib	Colorectal cancer	(57)
	RO4987655	Lung cancer	(94)
	TAK-733	Lung cancer	(95)
BRAF			
	PLX4720	Colorectal and melanoma	(58,59,96)
	PLX3603		
HDAC			
	Belinostat	Ovarian cancer	(68)
	Vorinostat	Colorectal cancer	(97)

Reversal of Drug Resistance

The clinical use of targeted anticancer agents significantly improved the outcome of cancer patients and became a valid therapeutic option for tumors with a known genetic profile and molecular landscape. However, despite the optimal initial response to therapy, the majority of patients invariably develop resistance to the targeted agent. Multiple molecular mechanisms may be responsible for the acquisition of drug resistance and include alterations of the target such as secondary mutations, reactivation of the signal transduction pathways in a parallel or serial mode, and alterations that drive prosurvival signals through different pathways. The elucidation of these mechanisms led to the development of new inhibitors that are able to overcome resistance in individual tumors. Preclinical testing of these inhibitors is required to prove their efficacy and to promote their use in clinical trials. Translational imaging may provide additional endpoints to evaluate the efficacy of these new compounds in animal models and to detect reversal of drug resistance.

Several imaging studies with ^{18}F-FLT were performed in animal models bearing NSCLC that were resistant to erlotinib for the presence of T790M secondary mutation in EGFR.[99–101] Usually, T790M mutation occurs in EGFR with activating mutations under the selective pressure of the drug and is found in almost 50% of resistant NSCLCs. The mutation substitutes the threonine residue with a bulky methionine so that the binding of gefitinib or erlotinib to the ATP pocket of EGFR can be altered because of steric hindrance or a reduced binding affinity. Second- and third-generation inhibitors similarly to gefitinib and erlotinib compete with ATP for the binding to the kinase domain of EGFR but unlike first-generation agents, their binding to the receptor is covalent and irreversible. To monitor reversal of T790M-mediated resistance by these agents, mice bearing resistant tumors with T790M mutation were subjected to PET scan with ^{18}F-FLT before and after 3 days treatment with erlotinib or irreversible EGFR inhibitors such as CL-387,785, and WZ4002.[100] Post-treatment PET scans showed a significant decrease of ^{18}F-FLT uptake in tumors of animals treated with irreversible inhibitors as compared to baseline scans, whereas an increase of tracer uptake was observed in animals treated with erlotinib (Fig. 2A). These findings indicated that imaging studies with ^{18}F-FLT were able to detect the successful reversal of T790M-mediated resistance by second- and third-generation EGFR inhibitors.

Another mechanism adopted by cancer cells to develop resistance to targeted therapies is the upregulation and/or activation of a protein that uses the same signaling pathways of the target. Despite drug-induced inhibition of the target, a parallel redundant signaling is mediated by an altered companion receptor and transduced to downstream pathways that remain persistently active. A paradigmatic example of this type of resistance is the amplification of MET oncogene in EGFR-mutant NSCLC. This alteration is clinically observed in up to 20% of NSCLCs that become resistant to gefitinib or erlotinib and causes reactivation of signaling cascade downstream EGFR despite its continuous inhibition by TKIs. Other known tyrosine kinase receptors that can be responsible for this type of resistance include HER2,[102] IGF-1R,[103] and Axl.[104]

In this context, preclinical imaging studies may help to monitor the effects of new compounds designed to overcome this type of resistance. Nude mice bearing NSCLCs with amplification of MET gene and wild-type EGFR were subjected to ^{18}F-FLT PET before and after treatment with escalating doses of the MET inhibitor crizotinib or erlotinib.[62] An early and significant decrease of ^{18}F-FLT uptake was found in tumors treated with crizotinib, whereas no significant reduction of tracer uptake was observed in animals treated with erlotinib (Fig. 2B). These imaging findings indicated the reversal of MET-mediated resistance and were confirmed by

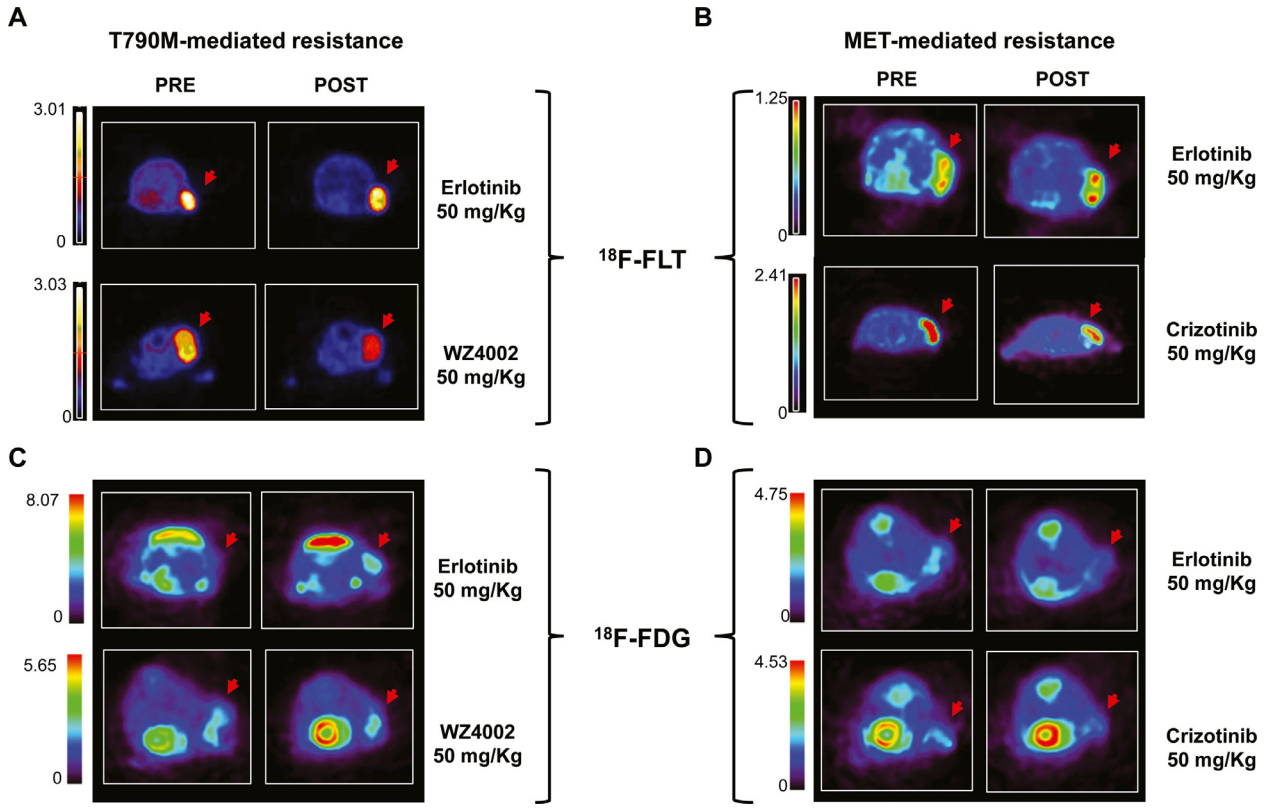

Figure 2 Monitoring reversal of drug resistance by ^{18}F-FLT and ^{18}F-FDG PET-CT. Representative transaxial PET images obtained from untreated and treated animals bearing resistant NSCLC harboring T790M mutation (H1975) (A, C) and MET amplification (H1993) (B, D). Mice were subjected to ^{18}F-FLT PET-CT (A, B) or ^{18}FDG PET-CT scan (C, D) at the baseline and after 3 days treatment with the following inhibitors: erlotinib, a reversible EGFR inhibitor; WZ4002, an irreversible EGFR inhibitor recognizing T790M mutant EGFR; crizotinib, a potent MET inhibitor. No changes or even an increase of ^{18}F-FLT uptake were observed after treatment with erlotinib confirming that tumors were resistant to this inhibitor. Conversely, both H1975 and H1993 xenografts showed a prompt reduction of ^{18}F-FLT uptake after treatment with WZ4002 or crizotinib, respectively. An increase of ^{18}F-FDG uptake was found in H1975 tumors after treatment with erlotinib, whereas a reduction of tracer uptake was observed in response to WZ4002. Conversely, in H1993 xenografts, ^{18}F-FDG uptake was reduced in response to both erlotinib and crizotinib. Modified from ref.[77].

the results of Ki67 staining of tumor sections that showed a significant decrease of the rate of proliferation in response to MET inhibitor but not to erlotinib.

As mentioned, caution should be used when interpreting ^{18}F-FDG scans performed very early in the course of treatment of resistant tumors with new reversal agents. Animal models of T790M- and MET-mediated resistance of NSCLC to EGFR TKIs were subjected to ^{18}F-FDG PET-CT scan before and 3 days after treatment with erlotinib, WZ4002 (targeting T790M mutation), crizotinib (targeting MET), or vehicle.[77] In models of T790M-mediated resistance, ^{18}F-FDG PET-CT scans showed reduction of ^{18}F-FDG uptake after treatment with WZ4002, whereas an increase of ^{18}F-FDG uptake was observed after treatment with erlotinib or vehicle. Conversely, in models of MET-mediated resistance, tumors showed a reduction of ^{18}F-FDG uptake after treatment with both crizotinib and erlotinib as well as an increase of tracer uptake in vehicle-treated animals. These findings indicated that ^{18}F-FDG uptake is a reliable imaging biomarker of T790M-mediated resistance and its reversal in NSCLC, whereas it may not be accurate in the detection of MET-mediated resistance. Figure 2C and D shows representative images of ^{18}F-FDG PET scan performed in animal models of T790M- and MET-mediated resistance to erlotinib treated with agents designed to overcome resistance.

Amplification or a mutation in genes of signaling mediators along the pathways driven by the oncoprotein is another adaptive mechanism causing resistance to targeted agents. For instance, BRAF mutations in the MAP kinase pathway cause resistance to EGFR inhibitors.[105] In a different cellular context, unresponsiveness of colon cancer to BRAF (V600E) inhibition is caused by a rapid feedback activation of EGFR that triggers continued proliferation even when BRAF (V600E) is inhibited.[106] This type of resistance can be circumvented by combining the inhibitor of the oncogene driver and the inhibitor of the adaptive mechanism. In this context, preclinical imaging can help to identify the best combination of drugs for a given mechanism of resistance.

Combined Therapies

The simultaneous inhibition of multiple signaling pathways emerged as a potentially effective strategy to obtain a durable

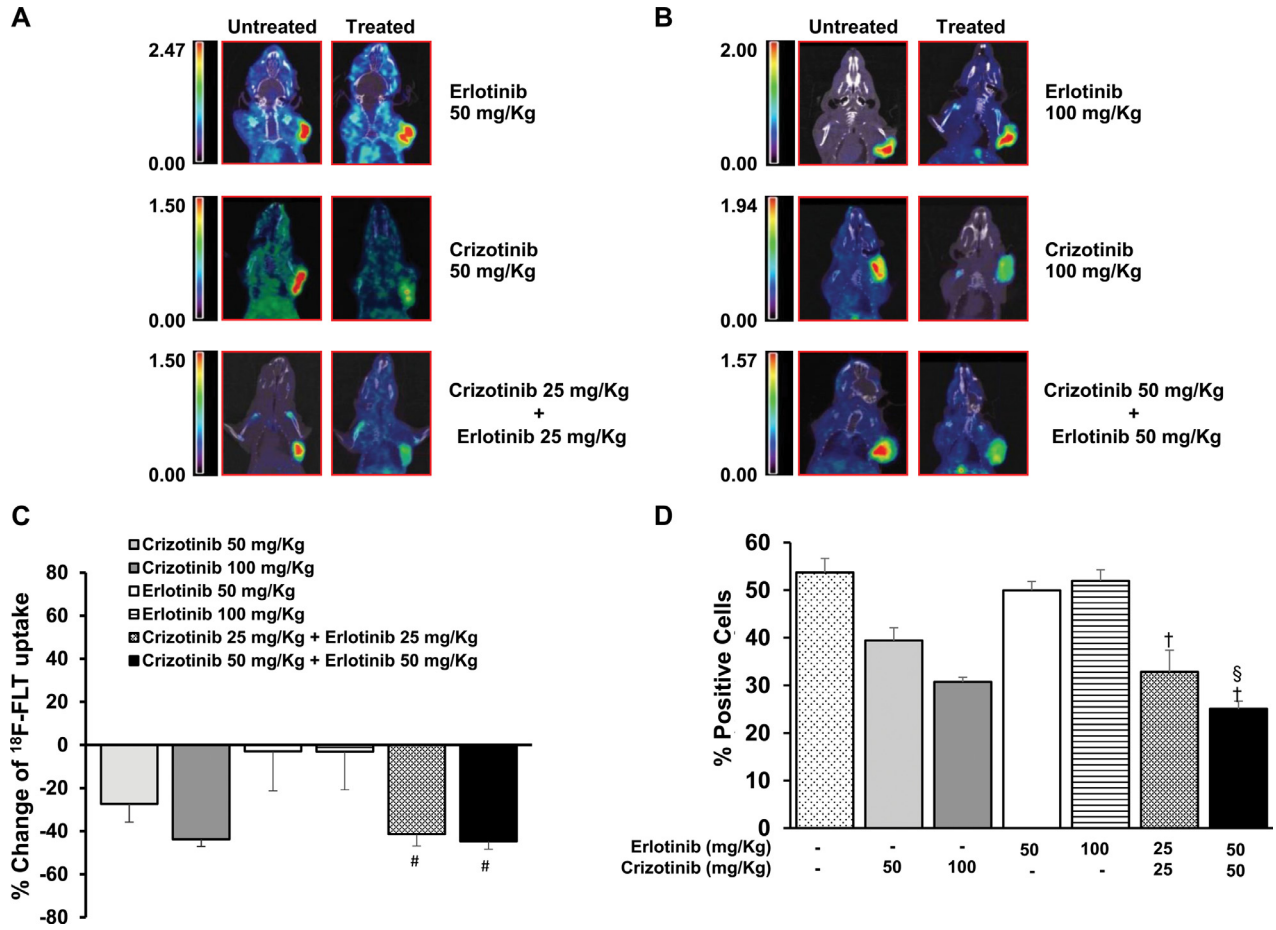

Figure 3 ^{18}F-FLT PET-CT for detection of drug synergy after combined therapies. Representative coronal fusion ^{18}F-FLT PET-CT images of mice bearing H1993 xenografts obtained at baseline and after 3 days treatment with erlotinib and crizotinib alone or in combination at a cumulative dose of 50 mg/kg (A) and 100 mg/kg (B). Treatment with erlotinib did not cause any change of ^{18}F-FLT uptake in tumors, whereas treatment with crizotinib showed a strong reduction of tracer uptake in xenografts. When combined treatment was administered to animals at cumulative doses equivalent to that of single agents, tumors showed a strong ^{18}F-FLT uptake reduction comparable to that caused by crizotinib alone at twofold higher dose as compared to combination indicating a drug synergy. (C) Percentage variations of ^{18}F-FLT uptake in H1993 tumor-bearing animals in response to treatment with single agent or with escalating dose of combined treatment. #, $P < 0.05$ combined treatment vs 50 mg/kg crizotinib. (D) Percentage of positive cells at Ki67 staining of tumor sections (§, $P < 0.05$ combined treatment vs 100 mg/kg crizotinib; †, $P < 0.05$ combined treatment vs 50 mg/kg crizotinib). Modified from ref.[107].

targeted therapeutic control of cancer in individual patients. The rational combination of two or more selective inhibitors is based on genomic profiling of single tumors or circulating tumor cells that may identify the oncogene driver and other key signaling mediators causing tumor relapse. Patient-derived xenografts or organoids may constitute an alternative in the future. In fact, growing tumor xenografts or organoids from single patient biopsies may allow to test the sensitivity of individual patients to targeted agents alone or in combination. In this context, preclinical imaging studies were performed to test whether noninvasive imaging with radiolabeled probes can detect the combined effects of targeted agents in animal models with a specific genetic signature. In these studies, the experimental design is challenging and several issues need to be addressed including the choice of the model, the selection of targeted agents, the starting dose of each drug and the cumulative dose of the combination, drug scheduling, toxicity of drug combination, the statistic power of the study, and validation of the results.

Imaging studies with ^{18}F-FLT PET-CT were performed in a model of NSCLC harboring MET amplification and wild-type EGFR, before and after treatment for 3 days with erlotinib and crizotinib alone or in combination.[107] Two dose regimens were used at 50 mg/kg and 100 mg/kg and the combination of the two agents was performed using a constant dose ratio of 1:1 so that the combined dose was equivalent to that of the single agent. Imaging studies showed a significant reduction of ^{18}F-FLT uptake in response to combined treatment with EGFR and MET inhibitors that was higher than that obtained with single agents (Fig. 3). Imaging findings were confirmed by Ki67 immunostaining on sections of surgical excised tumors and by analysis of signaling mediators in untreated and treated tumors. Furthermore, this study highlighted the role of inositol triphosphate

receptor type 3 and its interaction with K-Ras in the enhancement of the effects of drug combination.

In another study, proliferation and apoptosis were evaluated with ^{18}F-FLT and ^{18}F-ICMT-11, respectively, in nude mice bearing T790M resistant NSCLC after treatment with vehicle, cetuximab alone or in combination with gemcitabine.[108] ^{18}F-FLT uptake was significantly decreased after treatment with cetuximab, whereas ^{18}F-ICMT-11 was slightly increased after repeated doses of cetuximab. No significant variations of both ^{18}F-FLT and ^{18}F-ICMT-11 uptake were observed in animals treated with cetuximab alone as compared to those receiving drug combination with gemcitabine indicating the lack of a significant therapeutic benefit in combining gemcitabine with an effective dose of cetuximab.

A different imaging approach was used for testing the sequential combination of capecitabine and trifluridine/tipiracil in colon cancer.[109] Capecitabine causes its anticancer effects through inhibition of thymidylate synthase resulting in an upregulation of thymidine salvage pathway. Trifluridine is a thymidine analogue that enters cancer cells through the salvage pathway and when phosphorylated by thymidine kinase 1 can exert its cytotoxic action. Imaging with ^{18}F-FLT PET was performed before and after 2 and 4 days of treatment with capecitabine. ^{18}F-FLT uptake was increased on day 2 and showed a distinguishable decline on day 4 in all sensitive xenografts. No changes of ^{18}F-FLT uptake were observed in two resistant xenografts, whereas two additional resistant models showed a continuous increase of ^{18}F-FLT uptake on days 2 and 4. A synergy of the sequential drug combination was found only in mice showing an increased ^{18}F-FLT uptake after capecitabine treatment.

In a genetically engineered mouse model of NF1 mutant malignant peripheral nerve sheath tumors, simultaneous treatment with mTORC1 and MEK inhibitors showed an enhanced antitumor activity as compared to the effects of single agents and induced tumor regression.[110] NF1 mutations drive tumorigenesis through hyperactivations of RAS/RAF/MAPK and PI3K/AKT pathways. In the attempts to identify a pharmacodynamic marker of effective suppression of these pathways, the transcriptional profiles of tumors treated with vehicle, single agents, and drug combination were examined, and GLUT1 was identified as one of the uniquely suppressed gene in animals receiving drug combination. Imaging studies with ^{18}F-FDG performed before and 40 hours after treatment with drug combination showed a significant reduction of ^{18}F-FDG uptake as compared to controls that included animals treated with vehicle and single agents.

Targeting Immune Checkpoints

Immune checkpoint blockade has emerged as a new therapeutic option in cancer treatment showing long-term durable responses in a subset of patients within a broad range of malignancies including melanoma, non−small cell lung cancer, and urothelial cancer. The targets of this therapeutic approach are not the oncogene drivers orchestrating proliferation and survival of cancer cells but the drivers of immune evasion of cancer cells. Recognized drivers of immune evasion of cancer cells are programmed death-1 (PD-1), programmed death-1 ligand (PD-L1), and cytotoxic T-lymphocyte antigen 4 (CTLA-4). Inhibition of these immune checkpoints by specific antibodies restores the ability of T cells to recognize and destroy tumor cells. However, not all patients respond to immunotherapy and the accurate selection of patients that can benefit from this therapeutic approach may be challenging. Several potential biomarkers have been proposed including the pre-existence of CD8+ tumor-infiltrating lymphocytes, intratumoral PD-L1 expression, and mutational load but none of them can be considered an absolute selection criterion for therapy. For instance, elevated levels of PD-L1 in tumor biopsies were associated with increased response to immunotherapy in melanoma, NSCLC, and bladder cancer but not in squamous head and neck and renal cell carcinoma.[111] Furthermore, objective tumor response was also observed in a certain percentage of patients with PD-L1 negative tumors. Noninvasive imaging using antibody-based tracers recognizing immune checkpoints has the potential to detect and quantify the expression of these targets providing an imaging biomarker for patient selection and monitoring. This approach already reached the clinical stage with the first-in-human study using ^{89}Zr-atezolizumab in 22 patients with locally advanced or metastatic bladder cancer, non−small cell lung cancer or triple-negative breast cancer.[112] Tracer uptake was observed in tumor lesions and in lymphoid organs such as spleen and nonmalignant lymph nodes and corresponded to PD-L1 expression both in tumors and in various normal lymphoid tissues. Furthermore, tracer uptake was a strong predictor of response to atezolizumab treatment in terms of progression-free survival and overall survival.

This clinical approach was made possible by several preclinical studies that tested the ability of whole antibodies, engineered antibody fragments, and protein binders to target immune checkpoints in animal tumor models.[113−115] In these studies, PD-L1 was the most extensively studied target since it is expressed on the surface of tumor cells and antigen presenting cells. It should be noted that targeting immune checkpoints in animal models required great efforts and posed several challenges. For instance, when targeting PD-L1, the choice of the model, syngeneic or xenografts, may alter the biodistribution of the tracer due to its species specificity against the target. When immunocompetent mice are used, murine tumor cell lines should be inoculated and antibody-based tracers should have a murine origin. This may limit the transfer of knowledge from preclinical studies to clinical trials. Furthermore, caution should be used in competition experiments with in vivo administration of excess cold murine antibody since high doses of immunocheck point inhibitors may have major adverse effects. In the attempts to overcome some of these limitations, imaging studies were also performed in humanized mice that are obtained by transplanting human CD34+ hematopoietic stem cells in myeloablated recipient mice. Despite all these difficulties, preclinical studies were important to test the selectivity of the binding of new tracers and to prove the

concept that it is feasible to visualize the expression of immune checkpoints.

Conclusions

Preclinical imaging became a key tool in the translational process moving newly developed targeted anticancer agents from discovery to clinical applications. Remarkable efforts have been made for the development and validation of radiolabeled probes targeting oncogene drivers of specific tumors allowing the use of these tracers to identify patients who can benefit from treatment. Preclinical imaging studies tested the effective inhibition of the target and its downstream pathways by evaluating early changes in drug-modulated processes allowing the identification of sensitive and resistant tumors. Finally, previous studies provided evidence that preclinical imaging can monitor the reversal of drug resistance by targeted agents specifically designed to overcome resistance. In conclusion, preclinical imaging by intervening in all clinically relevant steps of targeted cancer therapies may contribute to accelerate clinical approval of targeted agents and provide imaging biomarkers for patient selection, early monitoring of drug effects, and reversal of drug resistance thus complementing the role of molecular, genetic, and histopathologic tests.

Acknowledgment

This work was partly supported by AIRC, Associazione Italiana per la Ricerca sul Cancro (project No. IG-17249) and a grant from Regione Campania SATIN Project 2018-2020.

References

1. Sharma SV, Settleman J: Oncogene addiction: Setting the stage for molecularly targeted cancer therapy. Genes Dev 21:3214-3231, 2007
2. Weinstein IB, Joe A: Oncogene addiction. Cancer Res 68:3077-3080, 2008
3. Banerji U, Workman P: Critical parameters in targeted drug development: The pharmacological audit trail. Semin Oncol 43:436-445, 2016
4. Hoelder S, Clarke PA, Workman P: Discovery of small molecule cancer drugs: Successes, challenges and opportunities. Mol Oncol 6:155-176, 2012
5. Dancey JE, Bedard PL, Onetto N, et al: The genetic basis for cancer treatment decisions. Cell 148:409-420, 2012
6. Dai D, Li XF, Wang J, et al: Predictive efficacy of (11)C-PD153035 PET imaging for EGFR-tyrosine kinase inhibitor sensitivity in non-small cell lung cancer patients. Int J Cancer 138:1003-1012, 2016
7. Abourbeh G, Itamar B, Salnikov O, et al: Identifying erlotinib-sensitive non-small cell lung carcinoma tumors in mice using [(11)C]erlotinib PET. EJNMMI Res 5:4, 2015
8. Memon AA, Jakobsen S, Dagnaes-Hansen F, et al: Positron emission tomography (PET) imaging with [11C]-labeled erlotinib: A micro-PET study on mice with lung tumor xenografts. Cancer Res 69:873-878, 2009
9. Petrulli JR, Sullivan JM, Zheng MQ, et al: Quantitative analysis of [11C]-erlotinib PET demonstrates specific binding for activating mutations of the EGFR kinase domain. Neoplasia 15:1347-1353, 2013
10. Su H, Seimbille Y, Ferl GZ, et al: Evaluation of [(18)F]gefitinib as a molecular imaging probe for the assessment of the epidermal growth factor receptor status in malignant tumors. Eur J Nucl Med Mol Imaging 35:1089-1099, 2008
11. Slobbe P, Windhorst AD, Stigter-van Walsum M, et al: A comparative PET imaging study with the reversible and irreversible EGFR tyrosine kinase inhibitors [(11)C]erlotinib and [(18)F]afatinib in lung cancer-bearing mice. EJNMMI Res 5:14, 2015
12. Ballard P, Yates JW, Yang Z, et al: Preclinical comparison of osimertinib with other EGFR-TKIs in EGFR-mutant NSCLC brain metastases models, and early evidence of clinical brain metastases activity. Clin Cancer Res 22:5130-5140, 2016
13. Yeh HH, Ogawa K, Balatoni J, et al: Molecular imaging of active mutant L858R EGF receptor (EGFR) kinase-expressing nonsmall cell lung carcinomas using PET-CT. Proc Natl Acad Sci U S A 108:1603-1608, 2011
14. Song Y, Xiao Z, Wang K, et al: Development and evaluation of (18)F-IRS for molecular imaging mutant EGF receptors in NSCLC. Sci Rep 7:3121, 2017
15. Sun X, Xiao Z, Chen G, et al: A PET imaging approach for determining EGFR mutation status for improved lung cancer patient management. Sci Transl Med 10:eann8840, 2018
16. Genne P, Berthet C, Raguin O, et al: Preclinical proof of concept for the first nanocyclix TKI-PET radiotracer targeting activated EGFR positive lung tumors [abstract]. Cancer Res 77:1875A, 2017
17. Dijkers ECF, Kosterink JGW, Rademaker AP, et al: Development and characterization of clinical-grade 89Zr-trastuzumab for HER2/neu immunoPET imaging. J Nucl Med 50:974-981, 2009
18. McKnight BN, Viola-Villegas NT: Monitoring Src status after dasatinib treatment in HER2+ breast cancer with (89)Zr-trastuzumab PET imaging. Breast Cancer Res 20:130, 2018
19. Bensch F, Brouwers AH, Lub-de Hooge MN, et al: (89)Zr-trastuzumab PET supports clinical decision making in breast cancer patients, when HER2 status cannot be determined by standard work up. Eur J Nucl Med Mol Imaging 45:2300-2306, 2018
20. Dehdashti F, Wu N, Bose R, et al: Evaluation of [(89)Zr]trastuzumab-PET/CT in differentiating HER2-positive from HER2-negative breast cancer. Breast Cancer Res Treat 169:523-530, 2018
21. O'Donoghue JA, Lewis JS, Pandit-Taskar N, et al: Pharmacokinetics, biodistribution, and radiation dosimetry for (89)Zr-trastuzumab in patients with esophagogastric cancer. J Nucl Med 59:161-166, 2018
22. Reddy S, Shaller CC, Doss M, et al: Evaluation of the anti-HER2 C6.5 diabody as a PET radiotracer to monitor HER2 status and predict response to trastuzumab treatment. Clin Cancer Res 17:1509-1520, 2011
23. Robinson MK, Doss M, Shaller C, et al: Quantitative immuno-positron emission tomography imaging of HER2-positive tumor xenografts with an iodine-124 labeled anti-HER2 diabody. Cancer Res 65:1471-1478, 2005
24. Olafsen T, Kenanova VE, Sundaresan G, et al: Optimizing radiolabeled engineered anti-p185HER2 antibody fragments for in vivo imaging. Cancer Res 65:5907-5916, 2005
25. Chan C, Scollard DA, McLarty K, et al: A comparison of 111In- or 64Cu-DOTA-trastuzumab Fab fragments for imaging subcutaneous HER2-positive tumor xenografts in athymic mice using microSPECT/CT or microPET/CT. EJNMMI Res 1:15, 2011
26. Kramer-Marek G, Bernardo M, Kiesewetter DO, et al: PET of HER2-positive pulmonary metastases with 18F-ZHER2:342 affibody in a murine model of breast cancer: comparison with 18F-FDG. J Nucl Med 53:939-946, 2012
27. Vaidyanathan G, McDougald D, Choi J, et al: Preclinical evaluation of 18F-labeled anti-HER2 nanobody conjugates for imaging HER2 receptor expression by immuno-PET. J Nucl Med 57:967-973, 2016
28. Xavier C, Blykers A, Vaneycken I, et al: (18)F-nanobody for PET imaging of HER2 overexpressing tumors. Nucl Med Biol 43:247-252, 2016
29. Xavier C, Vaneycken I, D'Huyvetter M, et al: Synthesis, preclinical validation, dosimetry, and toxicity of 68Ga-NOTA-anti-HER2 nanobodies for iPET imaging of HER2 receptor expression in cancer. J Nucl Med 54:776-784, 2013
30. Altai M, Strand J, Rosik D, et al: Influence of nuclides and chelators on imaging using affibody molecules: Comparative evaluation of recombinant affibody molecules site-specifically labeled with (6)(8)Ga and (1)(1)(1)In via maleimido derivatives of DOTA and NODAGA. Bioconjug Chem 24:1102-1109, 2013

31. Altai M, Wallberg H, Honarvar H, et al: 188Re-ZHER2:V2, a promising affibody-based targeting agent against HER2-expressing tumors: Preclinical assessment. J Nucl Med 55:1842-1848, 2014
32. D'Huyvetter M, De Vos J, Xavier C, et al: (131)I-labeled anti-HER2 camelid sdAb as a theranostic tool in cancer treatment. Clin Cancer Res 23:6616-6628, 2017
33. Salgia R: MET in lung cancer: Biomarker selection based on scientific rationale. Mol Cancer Ther 16:555-565, 2017
34. Albiges L, Guegan J, Le Formal A, et al: MET is a potential target across all papillary renal cell carcinomas: Results from a large molecular study of pRCC with CGH array and matching gene expression array. Clin Cancer Res 20:3411-3421, 2014
35. Kim HJ, Yoon A, Ryu JY, et al: c-MET as a potential therapeutic target in ovarian clear cell carcinoma. Sci Rep 6:38502, 2016
36. Jagoda EM, Lang L, Bhadrasetty V, et al: Immuno-PET of the hepatocyte growth factor receptor Met using the 1-armed antibody onartuzumab. J Nucl Med 53:1592-1600, 2012
37. Li K, Tavare R, Zettlitz KA, et al: Anti-MET immunoPET for non-small cell lung cancer using novel fully human antibody fragments. Mol Cancer Ther 13:2607-2617, 2014
38. Perk LR, Stigter-van Walsum M, Visser GW, et al: Quantitative PET imaging of Met-expressing human cancer xenografts with 89Zr-labelled monoclonal antibody DN30. Eur J Nucl Med Mol Imaging 35:1857-1867, 2008
39. Arulappu A, Battle M, Eisenblaetter M, et al: c-Met PET imaging detects early-stage locoregional recurrence of basal-like breast cancer. J Nucl Med 57:765-770, 2016
40. Jagoda EM, Bhattacharyya S, Kalen J, et al: Imaging the met receptor tyrosine kinase (Met) and assessing tumor responses to a met tyrosine kinase inhibitor in human xenograft mouse models with a [99mTc](AH-113018) or Cy 5** (AH-112543) labeled peptide. Mol Imaging 14:499-515, 2015
41. Terwisscha van Scheltinga AG, Lub-de Hooge MN, Hinner MJ, et al: In vivo visualization of MET tumor expression and anticalin biodistribution with the MET-specific anticalin 89Zr-PRS-110 PET tracer. J Nucl Med 55:665-671, 2014
42. Comoglio PM, Trusolino L, Boccaccio C: Known and novel roles of the MET oncogene in cancer: A coherent approach to targeted therapy. Nat Rev Cancer 18:341-358, 2018
43. Schelhaas S, Heinzmann K, Bollineni VR, et al: Preclinical applications of 3′-Deoxy-3′-[(18)F]fluorothymidine in oncology—A systematic review. Theranostics 7:40-50, 2017
44. Jensen MM, Kjaer A: Monitoring of anti-cancer treatment with (18)F-FDG and (18)F-FLT PET: A comprehensive review of pre-clinical studies. Am J Nucl Med Mol Imaging 5:431-456, 2015
45. Aide N, Kinross K, Cullinane C, et al: 18F-FLT PET as a surrogate marker of drug efficacy during mTOR inhibition by everolimus in a preclinical cisplatin-resistant ovarian tumor model. J Nucl Med 51:1559-1564, 2010
46. Honer M, Ebenhan T, Allegrini PR, et al: Anti-angiogenic/vascular effects of the mTOR inhibitor everolimus are not detectable by FDG/FLT-PET. Transl Oncol 3:264-275, 2010
47. Johnbeck CB, Munk Jensen M, Haagen Nielsen C, et al: 18F-FDG and 18F-FLT-PET imaging for monitoring everolimus effect on tumor-growth in neuroendocrine tumors: Studies in human tumor xenografts in mice. PLoS One 9:e91387, 2014
48. Li Z, Graf N, Herrmann K, et al: FLT-PET is superior to FDG-PET for very early response prediction in NPM-ALK-positive lymphoma treated with targeted therapy. Cancer Res 72:5014-5024, 2012
49. Fuereder T, Wanek T, Pflegerl P, et al: Gastric cancer growth control by BEZ235 in vivo does not correlate with PI3K/mTOR target inhibition but with [18F]FLT uptake. Clin Cancer Res 17:5322-5332, 2011
50. O'Halloran PJ, Viel T, Murray DW, et al: Mechanistic interrogation of combination bevacizumab/dual PI3K/mTOR inhibitor response in glioblastoma implementing novel MR and PET imaging biomarkers. Eur J Nucl Med Mol Imaging 43:1673-1683, 2016
51. Zhu Y, Tian T, Zou J, et al: Dual PI3K/mTOR inhibitor BEZ235 exerts extensive antitumor activity in HER2-positive gastric cancer. BMC Cancer 15:894, 2015
52. Keen HG, Ricketts SA, Maynard J, et al: Examining changes in [18 F]FDG and [18 F]FLT uptake in U87-MG glioma xenografts as early response biomarkers to treatment with the dual mTOR1/2 inhibitor AZD8055. Mol Imaging Biol 16:421-430, 2014
53. Saint-Hubert MD, Brepoels L, Devos E, et al: Molecular imaging of therapy response with (18)F-FLT and (18)F-FDG following cyclophosphamide and mTOR inhibition. Am J Nucl Med Mol Imaging 2:110-121, 2012
54. Haagensen EJ, Thomas HD, Wilson I, et al: The enhanced in vivo activity of the combination of a MEK and a PI3K inhibitor correlates with [18F]-FLT PET in human colorectal cancer xenograft tumour-bearing mice. PLoS One 8:e81763, 2013
55. Leyton J, Smith G, Lees M, et al: Noninvasive imaging of cell proliferation following mitogenic extracellular kinase inhibition by PD0325901. Mol Cancer Ther 7:3112-3121, 2008
56. Solit DB, Santos E, Pratilas CA, et al: 3′-deoxy-3′-[18F]fluorothymidine positron emission tomography is a sensitive method for imaging the response of BRAF-dependent tumors to MEK inhibition. Cancer Res 67:11463-11469, 2007
57. Honndorf VS, Schmidt H, Wiehr S, et al: The synergistic effect of selumetinib/docetaxel combination therapy monitored by [(18)F]FDG/[(18)F]FLT PET and diffusion-weighted magnetic resonance imaging in a colorectal tumor xenograft model. Mol Imaging Biol 18:249-257, 2016
58. Geven EJ, Evers S, Nayak TK, et al: Therapy response monitoring of the early effects of a new BRAF inhibitor on melanoma xenograft in mice: Evaluation of (18) F-FDG-PET and (18) F-FLT-PET. Contrast Media Mol Imaging 10:203-210, 2015
59. McKinley ET, Smith RA, Zhao P, et al: 3′-Deoxy-3′-18F-fluorothymidine PET predicts response to (V600E)BRAF-targeted therapy in preclinical models of colorectal cancer. J Nucl Med 54:424-430, 2013
60. McKinley ET, Zhao P, Coffey RJ, et al: 3′-Deoxy-3′-[18F]-fluorothymidine PET imaging reflects PI3K-mTOR-mediated pro-survival response to targeted therapy in colorectal cancer. PLoS One 9:e108193, 2014
61. Cullinane C, Dorow DS, Jackson S, et al: Differential (18)F-FDG and 3′-deoxy-3′-(18)F-fluorothymidine PET responses to pharmacologic inhibition of the c-MET receptor in preclinical tumor models. J Nucl Med 52:1261-1267, 2011
62. Iommelli F, De Rosa V, Gargiulo S, et al: Monitoring reversal of MET-mediated resistance to EGFR tyrosine kinase inhibitors in non-small cell lung cancer using 3′-deoxy-3′-[18F]-fluorothymidine positron emission tomography. Clin Cancer Res 20:4806-4815, 2014
63. Wiehr S, von Ahsen O, Rose L, et al: Preclinical evaluation of a novel c-Met inhibitor in a gastric cancer xenograft model using small animal PET. Mol Imaging Biol 15:203-211, 2013
64. Cullinane C, Waldeck KL, Binns D, et al: Preclinical FLT-PET and FDG-PET imaging of tumor response to the multi-targeted aurora B kinase inhibitor, TAK-901. Nucl Med Biol 41:148-154, 2014
65. Lee SJ, Kim EJ, Lee HJ, et al: A pilot study for the early assessment of the effects of BMS-754807 plus gefitinib in an H292 tumor model by [(18)F]fluorothymidine-positron emission tomography. Invest New Drugs 31:506-515, 2013
66. Moroz MA, Kochetkov T, Cai S, et al: Imaging colon cancer response following treatment with AZD1152: A preclinical analysis of [18F]fluoro-2-deoxyglucose and 3′-deoxy-3′-[18F]fluorothymidine imaging. Clin Cancer Res 17:1099-1110, 2011
67. Na YS, Jung KA, Kim SM, et al: The histone deacetylase inhibitor PXD101 increases the efficacy of irinotecan in in vitro and in vivo colon cancer models. Cancer Chemother Pharmacol 68:389-398, 2011
68. Jensen MM, Erichsen KD, Johnbeck CB, et al: [18F]FDG and [18F]FLT positron emission tomography imaging following treatment with belinostat in human ovary cancer xenografts in mice. BMC Cancer 13:168, 2013
69. Kaliszczak M, Trousil S, Aberg O, et al: A novel small molecule hydroxamate preferentially inhibits HDAC6 activity and tumour growth. Br J Cancer 108:342-350, 2013
70. Chan PC, Wu CY, Chou LS, et al: Monitoring tumor response after histone deacetylase inhibitor treatment using 3′-Deoxy-3′-[18F]-fluorothymidine PET. Mol Imaging Biol 17:394-402, 2015

71. Manning HC, Merchant NB, Foutch AC, et al: Molecular imaging of therapeutic response to epidermal growth factor receptor blockade in colorectal cancer. Clin Cancer Res 14:7413-7422, 2008
72. Leyton J, Alao JP, Da Costa M, et al: In vivo biological activity of the histone deacetylase inhibitor LAQ824 is detectable with 3′-deoxy-3′-[18F]fluorothymidine positron emission tomography. Cancer Res 66:7621-7629, 2006
73. Viel T, Boehm-Sturm P, Rapic S, et al: Non-invasive imaging of glioma vessel size and densities in correlation with tumour cell proliferation by small animal PET and MRI. Eur J Nucl Med Mol Imaging 40:1595-1606, 2013
74. McHugh CI, Lawhorn-Crews JM, Modi D, et al: Effects of capecitabine treatment on the uptake of thymidine analogs using exploratory PET imaging agents: (18)F-FAU, (18)F-FMAU, and (18)F-FLT. Cancer Imaging 16:34, 2016
75. Schelhaas S, Wachsmuth L, Hermann S, et al: Thymidine metabolism as a confounding factor for 3′-deoxy-3′-(18)F-fluorothymidine uptake after therapy in a colorectal cancer model. J Nucl Med 59:1063-1069, 2018
76. De Rosa V, Iommelli F, Monti M, et al: Reversal of Warburg effect and reactivation of oxidative phosphorylation by differential inhibition of EGFR signaling pathways in non-small cell lung cancer. Clin Cancer Res 21:5110-5120, 2015
77. De Rosa V, Iommelli F, Monti M, et al: Early 18F-FDG uptake as a reliable imaging biomarker of T790M-mediated resistance but not MET amplification in non-small cell lung cancer treated with EGFR tyrosine kinase inhibitors. EJNMMI Res 6:74, 2016
78. Venugopalan A, Lee MJ, Niu G, et al: EGFR-targeted therapy results in dramatic early lung tumor regression accompanied by imaging response and immune infiltration in EGFR mutant transgenic mouse models. Oncotarget 7:54137-54156, 2016
79. Vergez S, Delord JP, Thomas F, et al: Preclinical and clinical evidence that Deoxy-2-[18F]fluoro-D-glucose positron emission tomography with computed tomography is a reliable tool for the detection of early molecular responses to erlotinib in head and neck cancer. Clin Cancer Res 16:4434-4445, 2010
80. Su H, Bodenstein C, Dumont RA, et al: Monitoring tumor glucose utilization by positron emission tomography for the prediction of treatment response to epidermal growth factor receptor kinase inhibitors. Clin Cancer Res 12:5659-5667, 2006
81. Zhou LN, Wu N, Liang Y, et al: Monitoring response to gefitinib in nude mouse tumor xenografts by (18)F-FDG microPET-CT: Correlation between (18)F-FDG uptake and pathological response. World J Surg Oncol 13:111, 2015
82. Mignion L, Schmitz S, Michoux N, et al: 2′-deoxy-2′-[18F] fluoro-D-glucose positron emission tomography, diffusion-weighted magnetic resonance imaging, and choline spectroscopy to predict the activity of cetuximab in tumor xenografts derived from patients with squamous cell carcinoma of the head and neck. Oncotarget 9:28572-28585, 2018
83. Dorow DS, Cullinane C, Conus N, et al: Multi-tracer small animal PET imaging of the tumour response to the novel pan-Erb-B inhibitor CI-1033. Eur J Nucl Med Mol Imaging 33:441-452, 2006
84. Nielsen CH, Jensen MM, Kristensen LK, et al: In vivo imaging of therapy response to a novel pan-HER antibody mixture using FDG and FLT positron emission tomography. Oncotarget 6:37486-37499, 2015
85. Cullinane C, Dorow DS, Kansara M, et al: An in vivo tumor model exploiting metabolic response as a biomarker for targeted drug development. Cancer Res 65:9633-9636, 2005
86. Pantaleo MA, Nicoletti G, Nanni C, et al: Preclinical evaluation of KIT/PDGFRA and mTOR inhibitors in gastrointestinal stromal tumors using small animal FDG PET. J Exp Clin Cancer Res 29:173, 2010
87. Prenen H, Deroose C, Vermaelen P, et al: Establishment of a mouse gastrointestinal stromal tumour model and evaluation of response to imatinib by small animal positron emission tomography. Anticancer Res 26:1247-1252, 2006
88. Goggi JL, Bejot R, Moonshi SS, et al: Stratification of 18F-labeled PET imaging agents for the assessment of antiangiogenic therapy responses in tumors. J Nucl Med 54:1630-1636, 2013
89. Corroyer-Dulmont A, Peres EA, Petit E, et al: Detection of glioblastoma response to temozolomide combined with bevacizumab based on μMRI and μPET imaging reveals [18F]-fluoro-L-thymidine as an early and robust predictive marker for treatment efficacy. Neuro Oncol 15:41-56, 2013
90. Kristian A, Revheim ME, Qu H, et al: Dynamic (18)F-FDG-PET for monitoring treatment effect following anti-angiogenic therapy in triple-negative breast cancer xenografts. Acta Oncol 52:1566-1572, 2013
91. Meier R, Braren R, Kosanke Y, et al: Multimodality multiparametric imaging of early tumor response to a novel antiangiogenic therapy based on anticalins. PLoS One 9:e94972, 2014
92. Maynard J, Emmas SA, Ble FX, et al: The use of (18)F-fluorodeoxyglucose positron emission tomography ((18)F-FDG PET) as a pathway-specific biomarker with AZD8186, a PI3Kbeta/delta inhibitor. EJNMMI Res 6:62, 2016
93. Saint-Hubert MD, Devos E, Ibrahimi A, et al: Bioluminescence imaging of therapy response does not correlate with FDG-PET response in a mouse model of Burkitt lymphoma. Am J Nucl Med Mol Imaging 2:353-361, 2012
94. Tegnebratt T, Ruge E, Bader S, et al: Evaluation of efficacy of a new MEK inhibitor, RO4987655, in human tumor xenografts by [(18)F] FDG-PET imaging combined with proteomic approaches. EJNMMI Res 4:34, 2014
95. Ishino S, Miyake H, Vincent P, et al: Evaluation of the therapeutic efficacy of a MEK inhibitor (TAK-733) using (1)(8)F-fluorodeoxyglucose-positron emission tomography in the human lung xenograft model A549. Ann Nucl Med 29:613-620, 2015
96. Rohde S, Lindner T, Polei S, et al: Application of in vivo imaging techniques to monitor therapeutic efficiency of PLX4720 in an experimental model of microsatellite instable colorectal cancer. Oncotarget 8:69756-69767, 2017
97. Morelli MP, Tentler JJ, Kulikowski GN, et al: Preclinical activity of the rational combination of selumetinib (AZD6244) in combination with vorinostat in KRAS-mutant colorectal cancer models. Clin Cancer Res 18:1051-1062, 2012
98. McLarty K, Fasih A, Scollard DA, et al: 18F-FDG small-animal PET/CT differentiates trastuzumab-responsive from unresponsive human breast cancer xenografts in athymic mice. J Nucl Med 50:1848-1856, 2009
99. Ullrich RT, Zander T, Neumaier B, et al: Early detection of erlotinib treatment response in NSCLC by 3′-deoxy-3′-[F]-fluoro-L-thymidine ([F] FLT) positron emission tomography (PET). PLoS One 3:e3908, 2008
100. Zannetti A, Iommelli F, Speranza A, et al: 3′-deoxy-3′-18F-fluorothymidine PET/CT to guide therapy with epidermal growth factor receptor antagonists and Bcl-xL inhibitors in non-small cell lung cancer. J Nucl Med 53:443-450, 2012
101. Atkinson DM, Clarke MJ, Mladek AC, et al: Using fluorodeoxythymidine to monitor anti-EGFR inhibitor therapy in squamous cell carcinoma xenografts. Head Neck 30:790-799, 2008
102. Takezawa K, Pirazzoli V, Arcila ME, et al: HER2 amplification: A potential mechanism of acquired resistance to EGFR inhibition in EGFR-mutant lung cancers that lack the second-site EGFRT790M mutation. Cancer Discov 2:922-933, 2012
103. Cortot AB, Repellin CE, Shimamura T, et al: Resistance to irreversible EGF receptor tyrosine kinase inhibitors through a multistep mechanism involving the IGF1R pathway. Cancer Res 73:834-843, 2013
104. Zhang Z, Lee JC, Lin L, et al: Activation of the AXL kinase causes resistance to EGFR-targeted therapy in lung cancer. Nat Genet 44:852-860, 2012
105. Ohashi K, Sequist LV, Arcila ME, et al: Lung cancers with acquired resistance to EGFR inhibitors occasionally harbor BRAF gene mutations but lack mutations in KRAS, NRAS, or MEK1. Proc Natl Acad Sci U S A 109:E2127-E2133, 2012
106. Prahallad A, Sun C, Huang S, et al: Unresponsiveness of colon cancer to BRAF(V600E) inhibition through feedback activation of EGFR. Nature 483:100-103, 2012
107. Iommelli F, De Rosa V, Terlizzi C, et al: Inositol trisphosphate teceptor type 3-mediated enhancement of EGFR and MET cotargeting efficacy in non-small cell lung cancer detected by (18)F-fluorothymidine. Clin Cancer Res 24:3126-3136, 2018
108. Heinzmann K, Nguyen QD, Honess D, et al: Depicting changes in tumor biology in response to cetuximab monotherapy or

combination therapy by apoptosis and proliferation imaging using (18)F-ICMT-11 and (18)F-FLT PET. J Nucl Med 59:1558-1565, 2018

109. Kim SY, Jung JH, Lee HJ, et al: [(18)F]fluorothymidine PET informs the synergistic efficacy of capecitabine and trifluridine/tipiracil in colon cancer. Cancer Res 77:7120-7130, 2017
110. Malone CF, Fromm JA, Maertens O, et al: Defining key signaling nodes and therapeutic biomarkers in NF1-mutant cancers. Cancer Discov 4:1062-1073, 2014
111. Schalper KA, Kaftan E, Herbst RS: Predictive biomarkers for PD-1 axis therapies: The hidden treasure or a call for research. Clin Cancer Res 22:2102-2104, 2016
112. Bensch F, van der Veen EL, Lub-de Hooge MN, et al: (89)Zr-atezolizumab imaging as a non-invasive approach to assess clinical response to PD-L1 blockade in cancer. Nat Med 24:1852-1858, 2018
113. Mayer AT, Natarajan A, Gordon SR, et al: Practical immuno-PET radiotracer design considerations for human immune checkpoint imaging. J Nucl Med 58:538-546, 2017
114. Heskamp S, Hobo W, Molkenboer-Kuenen JD, et al: Noninvasive Imaging of tumor PD-L1 expression using radiolabeled anti-PD-L1 antibodies. Cancer Res 75:2928-2936, 2015
115. Maute RL, Gordon SR, Mayer AT, et al: Engineering high-affinity PD-1 variants for optimized immunotherapy and immuno-PET imaging. Proc Natl Acad Sci U S A 112:E6506-E6514, 2015